Komatiite from Eastern Iron Ore Group, Singhbhum Craton, India: Implication for Mantle Plume - Arc Tectonic Setting

Pawan Kumar Yadav[1], Manorama Das[2]

[1, 2]Geological Survey of India, SU: Bihar, Lohia Nagar, Kankarbagh, Patna – 800020, India

Abstract: ***In this paper, the field, petrographic and geochemical data of Patka komatiite belonging to the Badampahar Group of rocks in the Badampahar - Gorumahisani Greenstone Belt of the eastern Iron Ore Group of the Singhbhum Craton are presented for the first time which is mapped to the south of Patka village, Jharkhand. It is showing a similar history of sedimentation and volcanism in other contemporary Archaean greenstone belts of the world. Komatiites recently reported in some of them may hold key to the understanding of the early history of the evolution of the craton. The komatiite body (~600 m X ~250 m) trending N10ºW - S10ºE shows the concordant relationship with phyllites, amphibolite, and metachert which is underlain by phyllites, talc-tremolite-serpentine schist, and amphibolite and is overlain by metachert and quartzite. Spinifex, platy, and cumulate zones have been recorded in these komatiites. Petrographic study reveals that these komatiites contain tremolite, serpentine, magnetite, chlorite, and talc besides glass and rare skeletal olivine, clinopyroxene, and orthopyroxene. Alteration of the primary mineralogy (olivine and pyroxene) and relict glass to tremolite, serpentine, magnetite, chlorite, and talc is also observed. The igneous mineralogy has been altered during post-magmatic hydrothermal alteration processes corresponding metamorphism under greenschist to lower amphibolite facies. These komatiites are quit enriched in SiO_2: 37.56 - 42.79 wt. %, MgO: 24.78 - 33.36 wt. %, TiO_2: 0.18 - 0.49 wt. %, Al_2O_3/TiO_2: 8 - 30 and CaO/Al_2O_3: 0.49 - 1.79 and their Al2O3 contents (3.25 - 8.24 wt. %), $(Gd/Yb)_N$ (> 1.0), CaO/Al_2O_3 (> 1.0), Al_2O_3/TiO_2 (mostly < 18) and lower LREE and flat HREE fractionation patterns are comparable with those of the Al-depleted komatiites. In the Nb/Th vs. Zr/Nb diagram, these komatiites cluster away from the other volcanics, and in the Nb/Y vs. Zr/Y diagram they cluster between deep depleted mantle (DEP) and primitive mantle (PM). Bivariate plots of $(Gd/Yb)_N$ verse CaO/Al_2O_3 and Al_2O_3/TiO_2 imply varying degrees of involvement of garnet in the generation of komatiite melt in the mantle. The observed chemical characteristics indicate derivation of the komatiites magmas from different depths in a plume setting, whereas sub-contemporaneous felsic volcanism and TTG accretion can be attributed to an arc setting. In order to explain, the spatial association of komatiite volcanism with contemporaneous mafic-felsic volcanism and TTG accretion, we propose a combined mantle plume - arc setting with moderate contamination by continental crust or sub-continental lithosphere.***

Keywords: Komatiite, Geodynamic setting, Whole rock geochemistry, Badampahar-Gorumahisani greenstone belt (BGGB), Singhbhum Craton, India

1. Introduction

Komatiites, first identified by Viljoen & Viljoen (1969a) within the famous 3.5 Ga old Archaean greenstone belt of Barberton (Kaapvaal craton, South Africa) from their type locality along the Komati River. Komatiites are high-MgO (>18%), extrusive and ultramafic rocks (Arndt and Nisbet, 1982; Le Bas, 2000) which are mostly found in Archaean setup and rare or absent in the Proterozoic and Phanerozoic terrains. They form significant constituents of Archaean crust and are provided information key to the understanding of the composition and melting processes that operated in deep Archean mantle, continental growth rates, secondary processes such as metamorphism and fluid-induced alteration, geodynamic processes and crustal growth patterns. Detailed studies of komatiites have been done in the last four decades from several Archaean greenstone belts viz. Barberton, Commondale, South Africa; Sargur and Badampahar-Gorumahisani, India; Ball, Canada; Munro and Tisdale, Canada which have mainly been reported from different parts of the world like South Africa, Canada, Australia, Brazil, Finland, North China and India (Jahn et al., 1982; Gruau et al., 1987; Wilson and Carlson, 1989; Arndt, 1994, 2008; Lesher and Arndt, 1995; Xie et al., 1993, 2012; Bhattacharya et al.,1996; Arndt et al., 1997; De Wit and Ashwal, 1997; Fan and Kerrich, 1997; Grove et al., 1997; Parman et al., 1997; Sylvester et al., 1997; Kerrich et al., 1999; Polat et al., 1999; Sahu and Mukherjee., 2001; Chavagnac, 2004; Raul Minas and Jost, 2006; Jayananda et al., 2008; Bose, 2009; Zhai and Santosh, 2011; Dostal and Mueller, 2012; Furnes et al., 2012; Mazumder et al,. 2012a, b; Tushipokla and Jayananda, 2013; Chaudhuri et al., 2015, 2017; Yadav et al., 2015; Yadav et al., 2016; Yadav and Das, 2017a, b).

Speculation about geodynamics in greenstone belts of Archean and Proterozoic was tricky as tectonic processes and crust-mantle interaction of Archean was markedly different from the present and is still a topic of discussion of the geodynamic context of komatiite magma generation and eruption. Several models regarding the genesis and geodynamic setting of the komatiite magma have been proposed by many workers, as to whether they are related to melt derivation at great depth by a high degree (~30%) of melting caused by mantle plumes (Ohtani et al., 1989; Nisbet et al., 1993; Boehler et al., 1995; Herzberg, 1995; Arndt et al., 1997; Arndt, 2003; Kerrich and Xie, 2002; Arndt et al., 2008), partial melting of peridotite (Allegre, 1982; Arndt et al., 1998), an oceanic plateau originated from mantle plume (Kerr et al., 1996; Polat and Kerrich, 2000), melting of shallow / deep mantle (Grove et al., 1997; Parman et al., 1997, 2001; Polat et al., 1999; Arndt, 2003; Chavagnac, 2004; Berray et al., 2008) and a combined mantle plume-island arc environment (Puchtel et al., 1999) or a subduction zone (Parman et al., 1997, 2001; Grove et al., 1999; Grove and Parman, 2004).

In the Indian subcontinent, komatiites are predominantly reported from the Archaean Sargur, Holenarsipur and Chitradurga schist belts of the Dharwar craton, southern India (Viswanatha et al., 1977; Hussain and Naqvi, 1983; Srikantia and Bose, 1985; Radhakrishna and Naqvi, 1986; Charan et al., 1988; Venkatadasu et al., 1991; Devapriyan et al., 1994; Subba Rao and Naqvi, 1999; Jayananda et al., 2008; Tushipokla and Jayananda, 2013). In the Singhbhum Craton, occurrences of komatiites are mainly reported in the eastern Iron Ore Group (Bhattacharya et al., 1996; Sahu and Mukherjee, 2001; Bose, 2009; Chaudhuri et al., 2015, 2017; Yadav et al., 2015; Yadav et al., 2016; Yadav and Das, 2017a, b). In this contribution, field, petrographic, and whole-rock geochemical data are presented on the Patka komatiite of the BGGB and discuss their implication on the post-magmatic alteration processes, crustal contamination besides drawing hypothesis on possible geodynamic setting and composition of the mantle source.

Geological setting of the Singhbhum Craton and the area of study

The Geological setting of the area of study is mainly discussed into two parts i.e. (i) Iron Ore Group Supracrustals: their stratigraphic status and (ii) Badampahar - Gorumahisani greenstone belt (BGGB) which belongs to the Singhbhum Craton. The Singhbhum Craton (SC) is a polycyclic Archaean crustal block of Palaeo - Mesoarchean age which is bordered by Chhotanagpur Gneissic Complex to the north, Bastar Craton to west, Eastern Ghats Mobile Belt to the south and vast tract of alluvium to the east and is covering an area of about 10,000 km2 (Fig.1). The supracrustals of the Older Metamorphic Group (OMG), the oldest member of the SC, consisting of pelitic schist, arenite, para, and ortho- amphibolites are dated ~3.5 - 3.6 Ga (Saha, 1994; Misra et al., 1999; Mukhopadhyay, 2001; Misra, 2006). The OMG is intruded by Older Metamorphic Tonalite Gneiss (OMTG) which represents the first stable continental crust, is dated around 3.44 Ga (Goswami et al., 1995; Acharyya et al., 2010). Both the OMG and OMTG are intruded by an early phase of Singhbhum Granitoid which consists of five distinct plutons emplaced around 3.3 Ga (Misra et al,. 1999). Tait et al. (2011), Upadhyay et al. (2014), and Nelson et al. (2014) offer new-age data on various lithocomponents of the Singhbhum craton. Supracrustals of the Iron Ore Group (IOG) is represented by low-grade volcano-sedimentary successions comprising meta-volcanics, felsic and intermediate volcanics (Yadav and Das, 2019a; Yadav et al., 2020), ultramafics, spinifex textured peridotitic komatiite (Yadav et al., 2015, 2016; Chaudhuri et al., 2015, 2017; Yadav and Das, 2017a, b), quartz-pebble conglomerate (Yadav et al., 2016; Yadav and Das, 2017c, 2019b) quartzites, banded iron formation, metachert with minor carbonate rocks which occur as three detached belts along the periphery of the nucleus viz. Noamundi - Jamda - Koira belt (NJK belt), the western IOG; the southern IOG, Tomka - Daitari belt (TD belt), and the eastern IOG, the Badampahar - Gorumahisani belt (BG belt; Fig.1). The age relation between the three belts is not yet resolved and is a subject of debate. The relation between the IOG, OMG, OMTG, and the Singhbhum Granite is far from clear as can be construed from discussions in publications by Nelson et al., 2014 and Upadhyay et al., 2014.

(i) Iron Ore Group Supracrustals: their stratigraphic status

Some workers consider the IOG belts peripheral to the Singhbhum cratonic nucleus to be coeval, while others consider these to be of different ages (Saha, 1994). Many would agree the BGG belt extending southwards up to Hadgarh to be relatively the older amongst the three and some would even argue that this may be coeval with OMG supracrustals. Mukhopadhyay et al. (2008) consider the IOG greenstone sequence of the Tomka - Daitari belt as ~3.5 Ga old based on SHRIMP data on dacite occurring at its base. Volcano-sedimentary sequence in the Malayagiri basin is also considered as the equivalent of the IOG (Saha, 1994). Igneous crystallisation date of 2806±6 Ma from the dacitic tuff of the Malayagiri IOG basin, south of Palalahara was reported by Nelson et al., 2014 and they attributed that the sedimentary rocks of the IOG were deposited within different basins over an 800 million years interval. They also described a 5 stage-model of the evolution of the craton to account for the conflicting range of deposition ages so far obtained for the Iron Ore Group sedimentary rocks within the different basins. According to them, (a) the OMTG tonalites were emplaced between 3530 to 3300 Ma during the Stage 1 and were transformed into tonalite gneisses during Stage 2 at c. 3325 to 3300 Ma, (b) basalts, dacites and banded iron-formations deposited onto OMTG tonalite basement at c. 3507 Ma are now preserved within the southern (Tomka-Daitari) basin, (c) undeformed and unmetamorphosed OMG sedimentary rocks were preserved (as IOG cycle 1) around the margins of the newly-cratonised basement, (d) BIF and clastic sedimentary rocks were deposited around the margins of the craton onto the older sedimentary rocks and adjacent gneissic basement until c. 3.1 Ga (e) differentiated granitic rocks were emplaced during Stage 4, between 3.1 and 3.0 Ga, (f) sedimentary and volcanic rocks were deposited within the Malayagiri basin at 2.8 Ga, during Stage 5. Based on the above data, they interpreted that the sedimentary rocks of the eastern Iron Group i.e. Badampahar-Gorumahisani greenstone belt and lower part of the western Iron Group (Bonai-Keonjhar greenstone belt) were deposited simultaneously with those of the southern (Tomka-Daitari) basin, at 3507 Ma.

Upadhyay et al., 2014 also conclude a polycyclic evolution of the Paleo to Meso-Archean crust of the Singhbhum craton. According to them, the supracrustal rocks representing the IOG greenstone successions are older or of similar age as the OMTG and the Singhbhum Granite (SG) and arguments that the OMTG or the SG served as the basement for deposition of the IOG are untenable. They opine that the IOG greenstone sequences must have formed over an older crustal nucleus which is no longer preserved but the 3.61 Ga inherited zircons are the only possible remnants of this earlier crust. The petrology and geochemistry of mafic-ultramafic volcanics which constitute a significant component of the IOG supracrustals have been reviewed by Bose (2009). Komatiites have been reported from the Badampahar-Gorumahisani greenstone belt by Bhattacharya et al., 1996; Sahu and Mukherjee, 2001; Bose, 2009; Chaudhuri et al., 2015, 2017; Yadav et al., 2015, 2016; Yadav and Das, 2017a, b. In this context, the known occurrences of komatiites confined only to the BG greenstone belt out of all the IOG belts could be a feature significant enough to help decipher the evolution of the Singhbhum Craton.

(ii) Badampahar - Gorumahisani greenstone belt (BGGB)

The Badampahar - Gorumahisani greenstone belt (BGGB) of the IOG which extends from Rajnagar in south Singhbhum district, Jharkhand to the south of Jashipur in Mayurbhanj district, Odisha is disposed in the form of a 120 km long narrow arc (Jena and Behera, 1998). The northern 70 km stretch from Rajnagar up to Rairangapur has an NW - SE trend and the southern 50 km stretch trends NNE - SSW up to Jashipur. It has an average width of about 4 km attaining maximum width of 10 km in the Rairangapur - Bisoi sector. The BGGB has been assigned different stratigraphic nomenclature by different workers. It was designated as the Iron Ore Stage by Dunn, 1929; the Iron Ore Series by Jones, 1934; the Iron Ore Group by Sarkar and Saha, 1977 and Banerjee (1974) classified it as the Gorumahisani Group. Iyenger and Murthy (1982) designated the rocks of the belt as Badampahar Group and they suggested that together with the Koira Group forms the Iron Ore Supergroup. The BGGB classified under the Badampahar Group is mainly constituted of basic metavolcanics, small and narrow bodies of meta-ultramafites, acid metavolcanics (rhyodacite), and chemogenic metasediments including minor terrigenous components. BIF in form of banded magnetite quartzite (BMQ) is a conspicuous member in the southern part of the belt, where 2 - 3 bands of BMQ associated with supergene iron ores is exposed over a strike length of over 15 km in a linear tract from near Sulaipat in the NE to Badampahar and beyond in the SW. Metamorphosed basalt exhibits pillow structure at many places, especially in SE of Madansila and Hatia in the central part of the belt (Jena and Mohanty, 1989; Yadav et al., 2015). Variolitic structure appears in Kharkai River section and amygdular metabasalt with vesicles is preserved at a few places near Hatia and the western contact with granite in the Gorumahisani sector (Yadav et al., 2015). All these features indicate dominantly submarine volcanism with subaerial effusion (Sahoo et al., 2010). Locally exposed amphibolite, hornblende schist, chlorite schist, and phyllite are always confined to the marginal parts of the belt. Spinifex textured peridotitic komatiite (STPK), serpentinite, metapyroxenite and talc-tremolite-serpentine schist belongs to the meta-ultramafites. Volcanic agglomerates comprising platy fragments of basalt welded in tuffaceous material of acidic composition occur in the Gorumahisani hill.

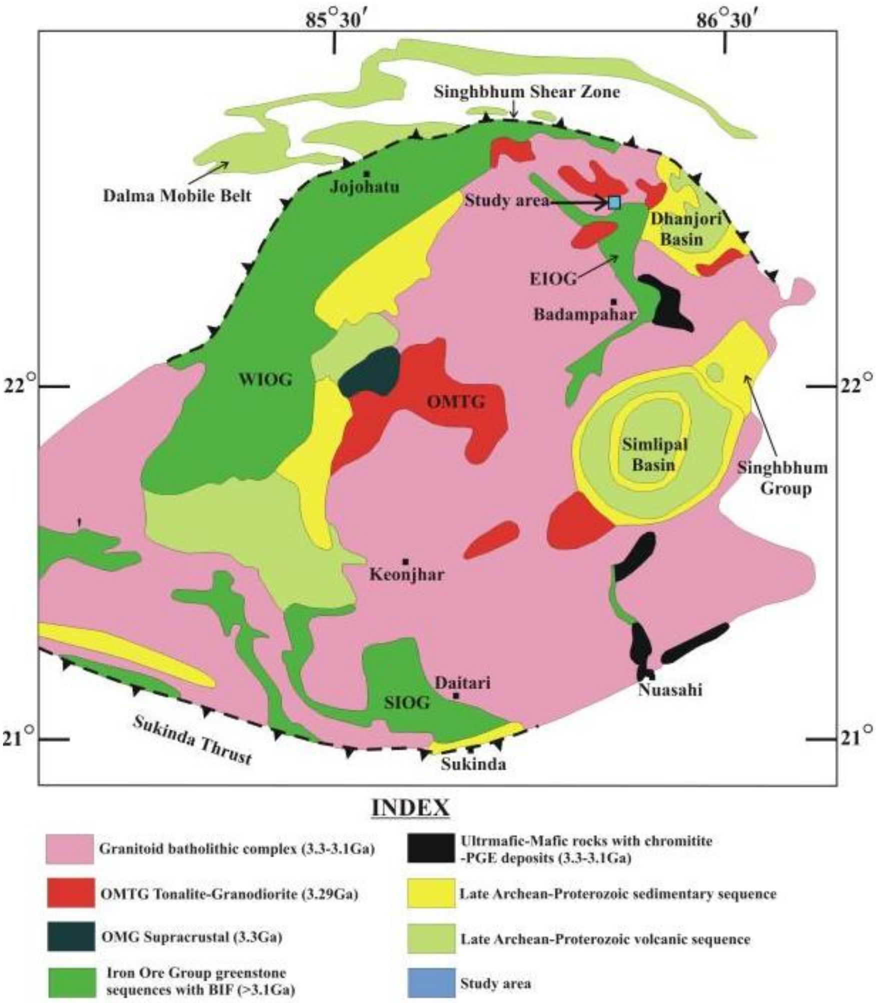

Figure 1: Generalized geological map of the Singhbhum Craton, north Odisha showing location of the study area (modified after Saha, 1994)

ISSN: 2319-7064
ResearchGate Impact Factor (2018): 0.28 | SJIF (2019): 7.583

Geology of the study area

A small body of komatiite was recorded towards the south of Patka, Jharkhand (22º36′40″ N: 86º13′34″ E, arrow Fig. 2). This segment of the BGG belt comprises a lithopackage of mafic-ultramafic rocks and the associated metasediments. The komatiite body (~600 m X ~250 m) trending N10ºW - S10ºE shows the concordant relationship with phyllites, amphibolite, and metachert. This komatiite is underlain by phyllites (Fig. 3a), talc-tremolite-serpentine schist, and amphibolite and is overlain by metachert (Fig. 3b) and quartzite. Patka komatiite display well preserved random spinifex zone (Fig. 3c & d), platy zone (Fig. 3e), and a well-developed cumulate zone (Fig. 3f). A common and distinctive texture of komatiite is known as spinifex texture which is defined by the criss-cross arrangement of olivine needles which are altered to serpentine, magnetite, chlorite, and tremolite. In this zone, the size of olivine needles varies from 5 mm to 5 cm in length and 2 mm to 5 mm in width respectively (Fig. 3c & d). In the platy zone, olivine plate size varies from 5 cm to 20 cm in length and 2 mm to 1 cm in width respectively (Fig. 3e). The very fine-grained groundmass of talc, chlorite, tremolite, serpentine and secondary magnetite is mostly occupied by the triangular and rectangular interspaces of the needles. At places, thin vein-lets of serpentine and cooling cracks are observed in the cumulate zone (Fig. 3f) and are also noticed in this komatiite. Olivine is replaced by serpentine, secondary magnetite, and talc, and pyroxenes are altered to tremolite, actinolite, chlorite, and epidote which indicate the assemblage of greenschist to lower amphibolite facies.

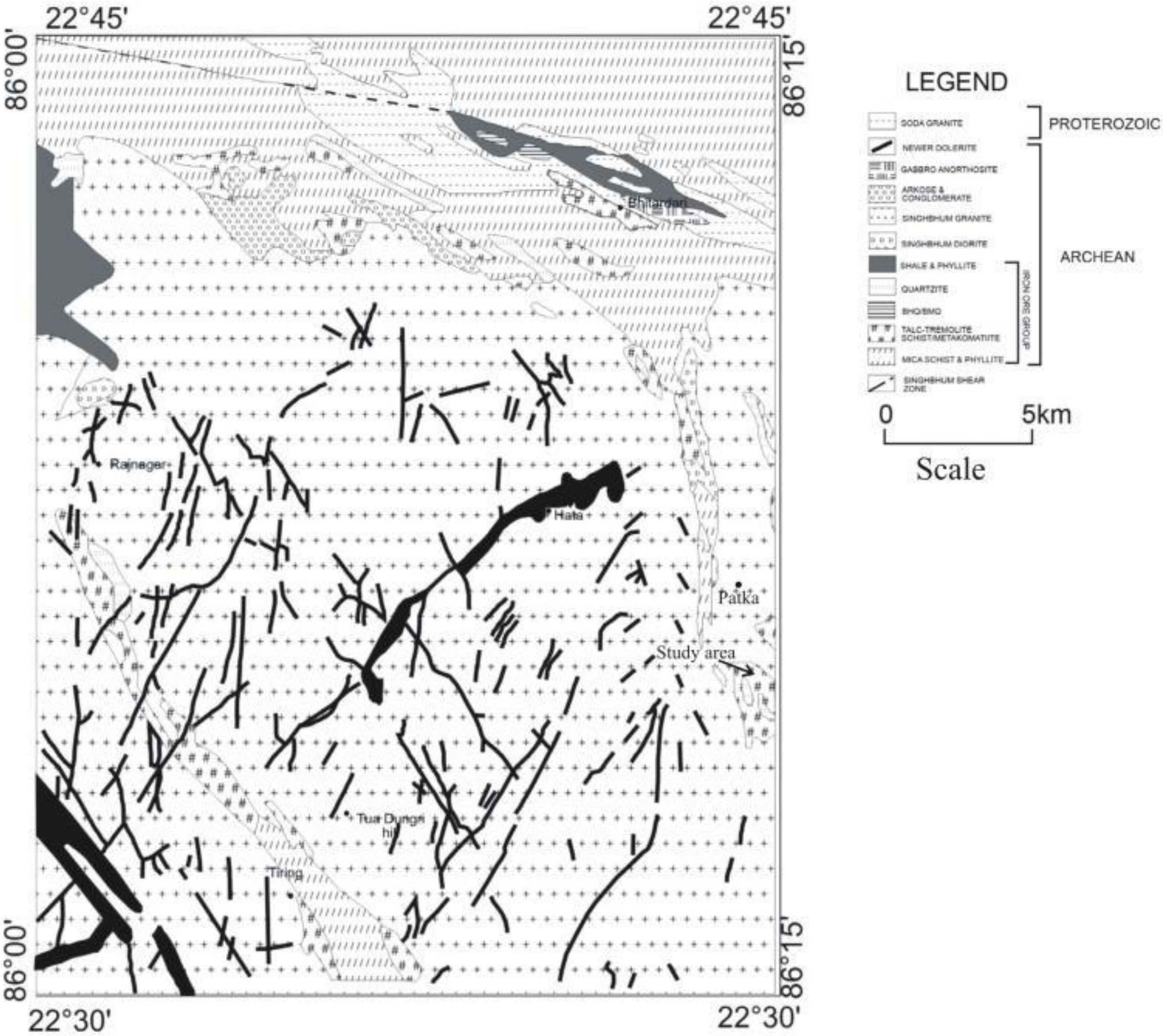

Figure 2: Geological map of the study area showing the occurrence of komatiite near Patka in the toposheet no. 73J/2 (available on www.gsi.gov.in).

Paper ID: SR20810161355 DOI: 10.21275/SR20810161355

Figure 3: (a) Foliation of phyllite is deformed and forms pucker folds. **(b)** Black metachert shows one set of prominent foliation. **(c & d)** Random spinifex zone displaying network of randomly orientated olivine needles. **(e)** Platy spinifex zone consists of parallel arrangement of olivine and pyroxene plates. **(f)** Thin vein-lets of serpentine are noticed in cumulate zone.

Petrography of komatiite

The studied komatiites show diverse petrographic characteristics in texture, primary mineralogy, and alteration features. They have been affected by greenschist to lower amphibolite facies of metamorphism. Komatiites are described for two distinct modes of occurrences viz. spinifex zone and cumulate zone in terms of mineralogy and texture under the optical microscope.

Komatiites show spectacular textures known as 'spinifex textures' which are defined by parallel or randomly oriented grouping of large skeletal plates of olivine crystals ranging from millimetres to centimetres and are embedded in a fine-grained groundmass of clinopyroxene, magnetite, and glass. The texture is explained by a magmatic quench crystallization effect promoted by the rapid cooling of melt with low nucleation rate and high growth rate of crystals at a large degree of supercooling. The zone exhibits both random (Fig. 4a & b) and platy spinifex (Fig. 4c & d) character. Olivine needles of random spinifex zone vary in size ranging from 10 mm to 15 cm in length and 1 mm to 5 mm in width respectively (Fig. 4a). Plates of olivine and clinopyroxenes in platy spinifex zone vary in length and width from 30 cm to 50 cm and 10 cm to 20 cm

Paper ID: SR20810161355 DOI: 10.21275/SR20810161355

respectively (Fig. 4c & d). The primary minerals like olivine and pyroxenes are mostly replaced by secondary minerals viz. serpentine, magnetite, chlorite, talc and tremolite. Out of the secondary phases, tremolite (>65 vol. %) is the most abundant mineral of this zone (Fig. 4b), followed by serpentine, magnetite, chlorite, and talc. Secondary magnetite is formed due to the breakdown of olivine and mostly occurs within the plates of olivine in feather-like shapes (Fig. 4a & c). The matrix of the spinifex zone is mostly formed by the anhedral shape of minerals like chlorite, serpentine, magnetite, and glass. The cumulate zone includes mainly tremolite, serpentine, olivine, augite, and enstatite as essential minerals. Magnetite, chlorite, and talc occur as accessories. It consists of pseudomorphic olivine replaced by serpentine (antigorite) and talc (Fig. 4e & f). The cumulate texture is defined by olivine pseudomorphs replaced by serpentine (antigorite) and secondary magnetite (Fig. 4e), whereas, inter-cumulus space is occupied by tremolite, serpentine and secondary magnetite (Fig. 4e). The relict grains of olivine are still preserved within the felted mass of serpentine and magnetite forming a mesh texture (Fig. 4e & f).

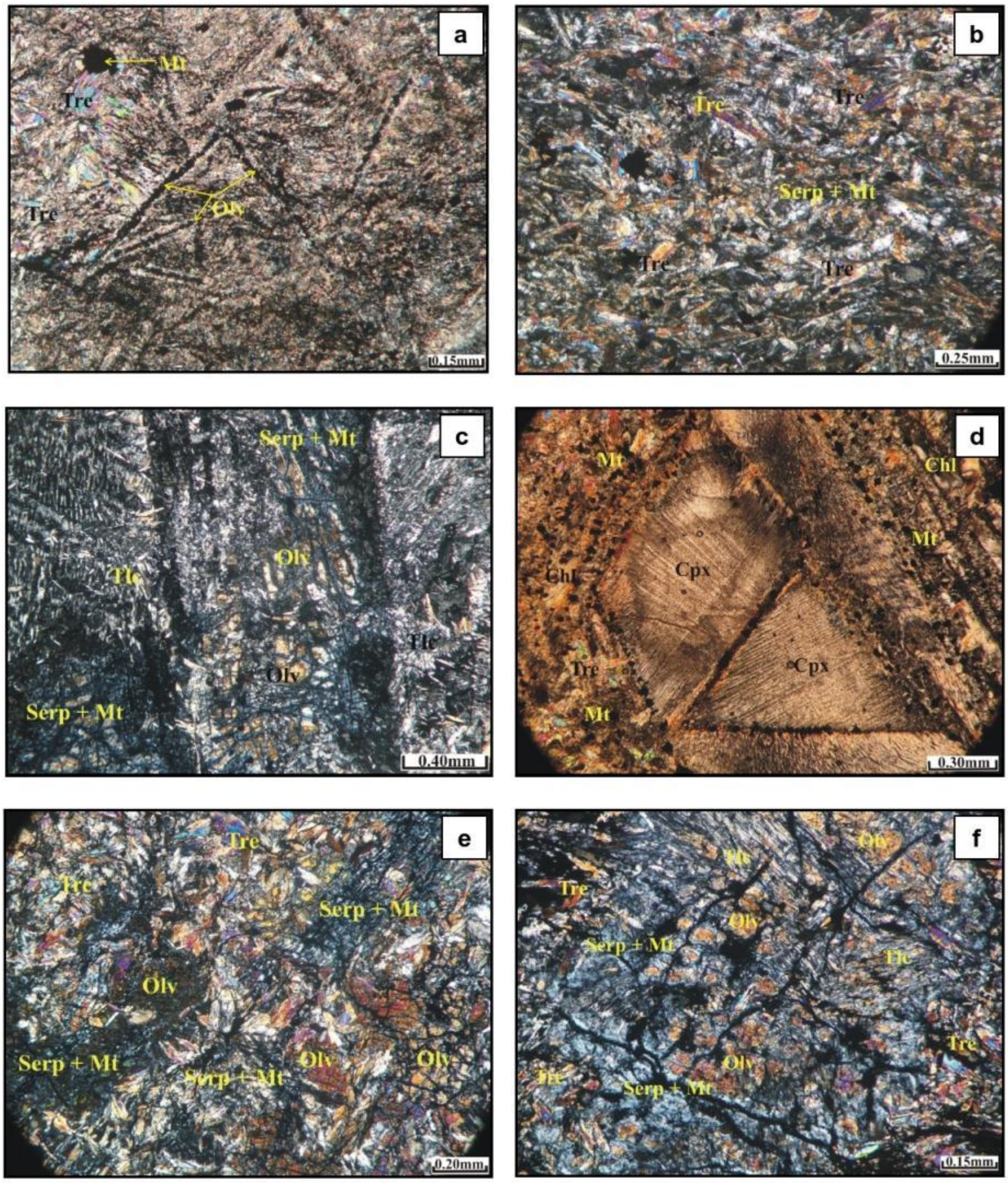

Figure 4: (a to d) Photomicrographs of spinifex zone. **(a)** Criss-cross arrangement of serpentine and tremolite needles **(b)** Needles of tremolite shows randomly orientations. **(c)** Large olivine plates are replaced by serpentine and secondary magnetite **(d)** Plates of pyroxenes (clinopyroxenes) are altered to tremolite and magnetite. **(e)** Cumulate zone shows cumulus (Olv) and inter-cumulus (Tre) textures. **(f)** Cumulate zone displaying relict grains of olivine, serpentine and magnetite forming mesh texture. **Abbreviations:** Olv, Olivine; Serp, Serpentine; Mt, Magnetite; Tre, Tremolite; Cpx, Clinopyroxene; Chl, Chlorite; Tlc, Talc.

Analytical techniques

Fourteen nos. of representative samples of komatiites from the from Badampahar - Gorumahisani greenstone belt, Singhbhum Craton were analysed for major-element oxides by X-ray Fluorescene (XRF) technique and trace elements and REE were analysed by Inductively Coupled Plasma Mass Spectrometer (ICP-MS) at the Eastern Region Laboratory, Kolkata, India. The analytical data is furnished in Table - 1.

2. Results and Discussion

Geochemical characteristics of komatiite

Patka samples are showing komatiitic in composition, with MgO content ranging from 24.78 to 28.61 wt. % in the spinifex zone and 30.84 - 33.36 wt. % in the cumulate zone. The range of the SiO_2 contents in the komatiite samples varies from 37.56 to 42.79 wt. %. The Al_2O_3/TiO_2 ratio which varies from 8.65 to 30.47 in the spinifex zone and from 9.18 to 24.56 in the cumulate zone. Besides, Ca-rich character indicated from the CaO/Al_2O_3 ratio (0.49 - 1.79) is very similar to that of the Al-depleted Barberton type komatiites (Viljoen and Viljoen, 1969a; Nesbitt et al., 1979, 1982; Jahn et al., 1982; Bickle et al., 1993; Lahaye and Arndt, 1996; Arndt et al., 2008). The presence of mainly hydrous minerals like tremolite, serpentine, talc, and chlorite are noticed in this unit which is attributed to a large variation in LOI wt. % ranging from 5.05 to 10.45 wt. %. Arndt and Nisbet, 1982 proposed a diagram based on MgO contents which show the distinction between komatiites and komatiitic basalts. The analysed samples are plotted in the triangular diagram of CaO-MgO-Al_2O_3 in which all samples are classified as komatiites (Fig. 5). In the binary variation diagrams of major elements oxides, a moderate to strong negative correlation has been observed in MgO versus SiO_2, Al_2O_3, Fe_2O_3, Na_2O, and K_2O. Plots of CaO and LOI show positive correlation and TiO2 reveals scattering. Expectedly, LOI displays a strong positive correlation with MgO, possibly a mark of susceptibility to alteration of Mg-Ca-rich minerals to secondary hydrous phases (Fig. 6). The trace element of komatiite samples shows significant contrast mainly in the Ni content of the spinifex zone ranging from 853 to1482 ppm and cumulate zone varying from 1127 to1617 ppm-respectively. Spinifex zone shows a slightly higher value of Cr (1839 - 3988 ppm) than the cumulate zone (1529 - 3250 ppm). The plot of Ni displays a strong positive correlation with MgO suggesting olivine fractionation (Arndt et. al., 2008). Plots of Cr, Sc, V, and Zr reveal a moderate negative correlation with MgO and Co, Rb, and Y display scattering (Fig. 7). Komatiites are enriched in LREE than HREE and the value of ΣREE varies from 7.45 to 55.32 ppm. Chondrite normalised REE fractionation patterns (Fig. 8a) reveal a slight enrichment of LREE compared with HREE anomalies (Nakumura, 1974; Table 1) and it shows wide variation in ratios of $(La/Sm)_N$: (0.65 - 3.2) and $(Gd/Yb)_N$: (0.73 - 1.59). In primitive mantle-normalised multi-element spider diagram, komatiites show relative enrichment of U, Pb, and Y and depletion in Ba, Sr, and Zr values (Fig. 8b). Major element ratios such as CaO/Al_2O_3 and Al_2O_3/TiO_2 in combination with $(Gd/Yb)_N$ values have been used to understand the nature of mantle source and garnet fractionation (Jahn et al., 1982; Cattell and Arndt, 1987; Gruau et al., 1987; Ohtani et al., 1989; Xie et al., 1993). Most of the $(Gd/Yb)_N$ versus CaO/Al_2O_3 and Al_2O_3/TiO_2 plots fall in the field of 'Garnet Fractionation' (Fig. 8c & d; Jahn et al., 1982; Arndt, 2003).

Table 1: Major elements (wt. %) and trace elements (ppm) data of komatiites from Badampahar - Gorumahisani greenstone belt, Singhbhum Craton

Sample No.	LK-1	LK-2	LK-3	LK-4	LK-5	LK-6	LK-7	LK-8	LK-9	LK-10	LK-11	LK-12	LK-13	LK-14
SiO_2	39.41	42.06	41.49	40.79	42.17	40.91	37.56	42.79	40.09	38.98	39.19	41.38	41.67	38.81
Al_2O_3	3.58	6.26	3.98	3.25	3.85	6.95	8.24	6.40	7.19	7.86	7.60	3.93	6.42	5.99
Fe_2O_3	12.42	11.63	13.77	8.70	9.91	13.52	14.28	10.37	13.13	14.39	12.90	7.16	9.63	9.18
MnO	0.22	0.26	0.22	0.13	0.19	0.20	0.17	0.21	0.18	0.18	0.21	0.15	0.14	0.19
MgO	31.53	26.52	26.15	33.36	31.56	26.78	27.65	25.72	27.93	24.78	26.57	33.20	28.61	30.84
CaO	4.05	7.08	7.11	4.96	3.80	4.82	4.06	7.34	4.34	4.10	3.81	3.58	5.31	6.03
Na_2O	0.03	0.31	0.23	0.13	0.06	0.22	0.18	0.25	0.24	0.26	0.24	0.06	0.09	0.09
K_2O	0.01	0.04	0.04	0.05	0.02	0.02	0.02	0.04	0.04	0.05	0.06	0.02	0.01	0.03
TiO_2	0.39	0.24	0.46	0.18	0.20	0.44	0.49	0.21	0.47	0.53	0.45	0.16	0.24	0.27
P_2O_5	0.02	0.03	0.03	0.01	0.02	0.10	0.35	0.01	0.25	0.31	0.05	0.01	0.01	0.07
LOI	8.43	5.05	5.68	9.12	8.22	6.50	7.03	6.62	6.52	8.69	8.99	10.45	7.9	8.63
Total	**100.09**	**99.48**	**99.16**	**100.6**	**100**	**100.4**	**100**	**99.96**	**100.3**	**100.1**	**100**	**100.1**	**100.0**	**100.1**
Ba	10	15	10	<20	73	49	58	20	95	21	115	55	14	16
Co	111	107	113	87	101	103	111	100	108	106	102	83	78	115
Cr	1529	3613	1839	2376	2931	3132	2955	3988	3070	2568	2514	3074	3438	3250
Cu	16	88	33	28	18	28	15	30	53	104	21	<5	9	551
Nb	2.5	5	2	5	5	5	5	4	5	5	5	5	5	5
Ni	1727	1122	1482	1617	1803	1026	953	1254	906	940	853	1600	1374	1127
Pb	<5	<5	6	6	<5	<5	<5	<5	<5	<5	6	<5	<5	5
Rb	4	2	3	5	6	9	7	3.6	8	9	9	8	9	7
Sc	12	28	23	13	11	28	27	26	26	35	31	15	27	30
Sr	31	65	43	41	16	9	18	59	16	17	11	12	10	23
Th	2.1	1.5	2	4	4	4	4	2.1	4	4	4	4	4	4
U	3.2	2	2.1	4	4	4	4	2.8	4	4	4	4	4	4
V	102	118	116	104	114	226	253	112	211	242	185	106	119	152
Y	12	12	15	9	11	16	28	11	21	24	13	9	9	11

Zr	24	23	32	11	11	48	59	19	46	58	47	9	9	12
La	0.88	8.27	1.91	0.76	0.78	1.86	4.84	1.42	3.63	6.72	4.72	2.33	2.01	4.07
Ce	2.76	17.44	6.04	1.76	1.82	4.32	14.57	5.17	9.76	18.89	11.57	5.62	4.23	9.58
Pr	0.46	1.95	0.67	0.21	0.18	0.64	1.84	0.45	1.27	2.53	1.17	0.62	0.56	1.13
Nd	2.54	7.62	3.34	1.00	0.96	3.12	9.58	2.04	6.47	11.27	4.77	2.51	2.20	4.62
Sm	0.83	1.59	1.01	0.35	0.32	2.12	2.98	0.58	1.95	2.91	1.19	0.60	0.59	1.10
Eu	0.27	0.24	0.24	0.22	0.14	0.2	0.63	0.17	0.39	0.53	0.24	0.14	0.15	0.19
Gd	0.9	1.57	1.61	0.64	0.60	1.51	4.41	0.9	2.95	3.34	1.21	0.67	0.76	1.24
Tb	0.18	0.28	0.3	0.13	0.12	0.4	0.80	0.16	0.57	0.72	0.27	0.16	0.20	0.30
Dy	0.87	1.34	1.93	0.82	0.88	1.12	4.93	0.96	3.48	3.72	1.40	0.80	1.11	1.61
Ho	0.19	0.29	0.43	0.19	0.18	0.45	1.02	0.2	0.75	0.81	0.30	0.19	0.26	0.35
Er	0.36	0.64	1.3	0.56	0.65	1.23	2.93	0.69	2.24	1.60	0.65	0.39	0.55	0.79
Tm	0.09	0.15	0.2	0.10	0.10	0.11	0.42	0.1	0.33	0.34	0.16	0.10	0.14	0.18
Yb	0.45	0.8	1.21	0.61	0.65	1.31	2.21	0.62	1.87	1.69	0.90	0.55	0.80	0.97
Lu	0.07	0.14	0.19	0.11	0.11	0.15	0.32	0.11	0.29	0.25	0.15	0.09	0.13	0.16
ΣREE	**10.85**	**42.32**	**20.38**	**7.45**	**7.47**	**18.54**	**51.49**	**13.57**	**35.95**	**55.32**	**28.69**	**14.76**	**13.67**	**26.26**
Fe2O3/(Fe2O3 + MgO)	0.28	0.3	0.34	0.21	0.24	0.34	0.34	0.29	0.32	0.37	0.33	0.18	0.25	0.23
Al2O3/ TiO2	9.18	26.08	8.65	18.05	19.25	15.79	16.81	30.47	15.29	14.83	16.89	24.56	26.75	22.18
CaO/Al2O3	1.13	1.13	1.79	1.53	0.99	0.69	0.49	1.15	0.6	0.52	0.5	0.91	0.83	1
Nb/U	0.78	2.5	0.95	1.25	1.25	1.25	1.25	1.43	1.25	1.25	1.25	1.25	1.25	1.25
Nb/Th	1.19	3.33	1	1.25	1.25	1.25	1.25	1.9	1.25	1.25	1.25	1.25	1.25	1.25
Zr/Nb	9.6	4.6	16	2.2	2.2	9.6	11.8	4.75	9.2	11.6	9.4	1.8	1.8	2.4
Nb/Y	0.21	0.42	0.13	0.56	0.45	0.31	0.18	0.36	0.24	0.21	0.38	0.56	0.56	0.45
Zr/Y	2	1.92	2.13	1.22	1	3	2.11	1.72	2.19	2.42	3.62	1	1	1.09
Nb/La	2.84	0.6	1.05	6.58	6.41	2.69	1.03	2.82	1.38	0.74	1.06	2.15	2.49	1.23
(La/Yb)N	1.3	6.89	1.05	0.83	0.79	1.05	1.46	1.53	1.3	2.65	3.48	2.84	1.67	2.81
(La/Sm)N	0.65	3.2	1.16	1.34	1.5	1.17	1	1.51	1.15	1.42	2.45	2.38	2.09	2.28
(Gd/Yb)N	1.59	1.56	1.06	0.84	0.73	1.02	1.59	1.16	1.26	1.58	1.07	0.97	0.75	1.03

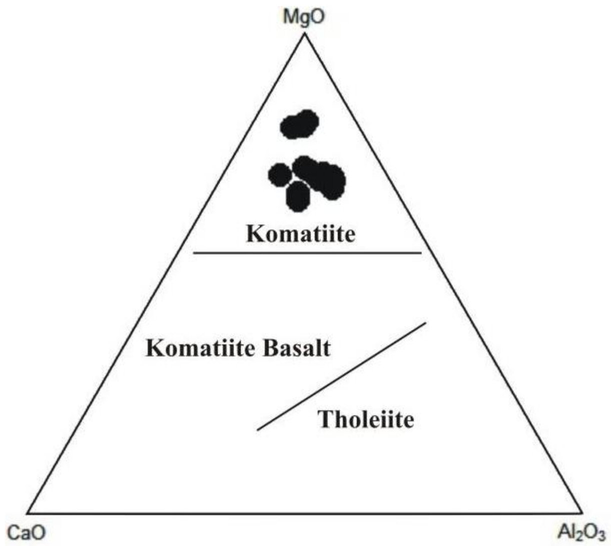

Figure 5: Plots in the CaO-MgO-Al_2O_3 diagram (Viljoen et al., 1982).

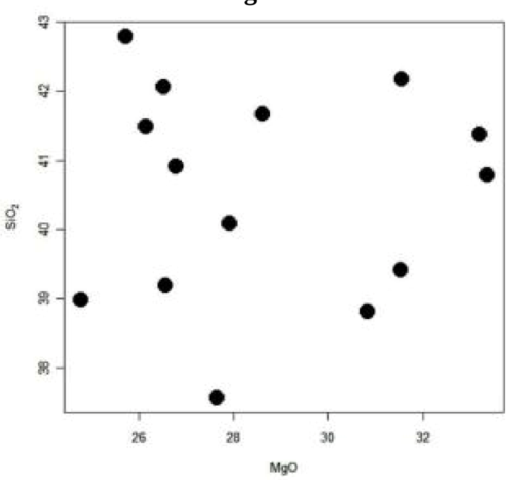

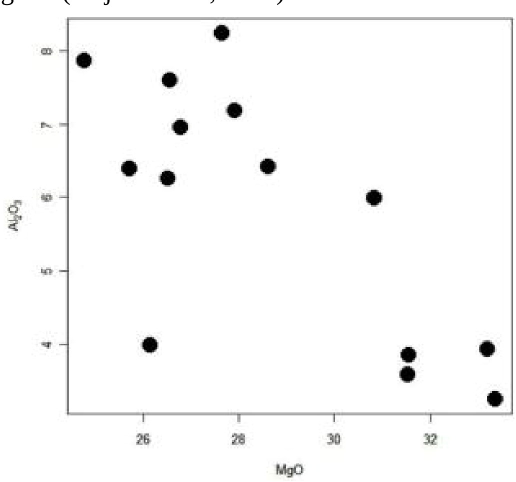

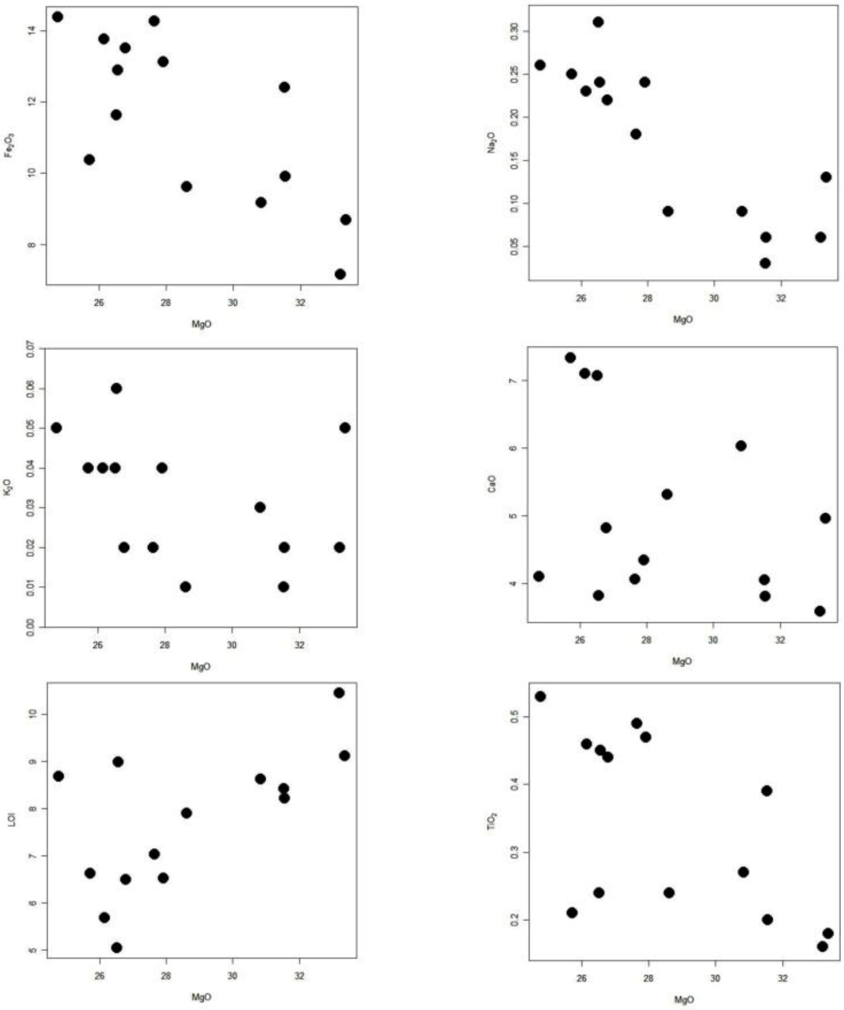

Figure 6: Plots of komatiites in variation diagrams for selected major oxides plotted against MgO.

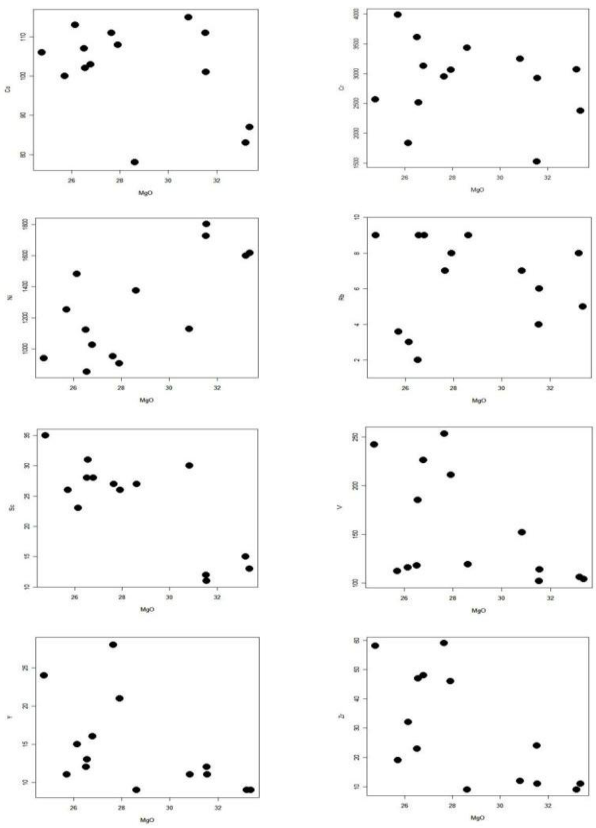

Figure 7: Variation diagrams for selected trace elements of komatiites plotted with MgO.

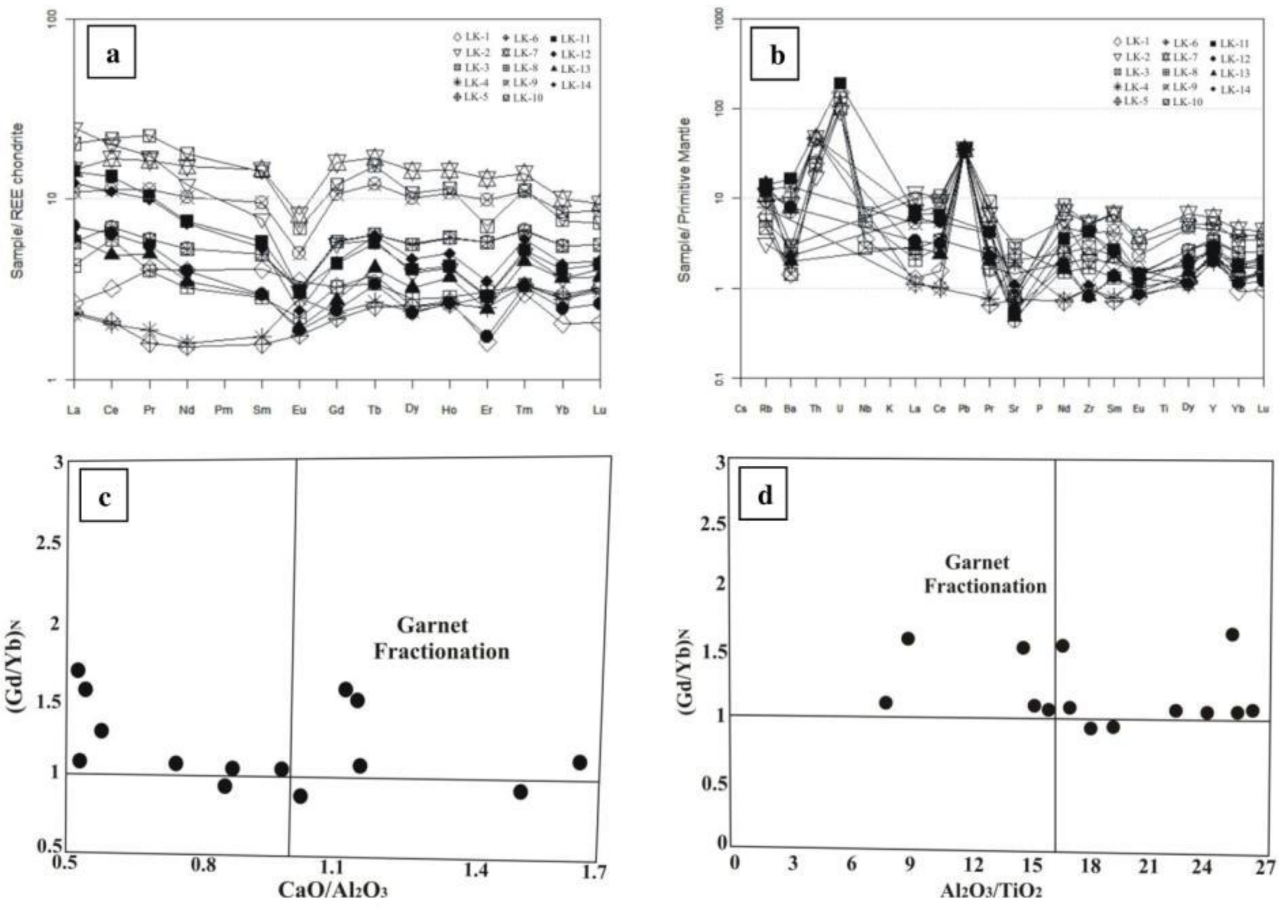

Figure 8: (a) Chondrite normalised REE plot of Patka komatiites. **(b)** Primitive mantle normalized multi-element diagram of komatiites (Sun and McDonough, 1989). **(c & d)** Samples of komatiites are plotted in $(Gd/Yb)_N$ ratios vs. CaO/Al_2O_3 and Al_2O_3/TiO_2 diagrams in which mostly samples falls in the garnet fractionation field.

Alteration or element mobility, metamorphism, and crustal contamination

Mobility of LILE and REE controlled by secondary processes such as induced hydrothermal alteration/element mobility and metamorphism in most Archaean komatiites of the different greenstone belts across the world has been well documented by Tourpin et al., 1991; Gruau et al., 1992 and Chavagnac, 2004. The Patka komatiites samples of BGGB comprising predominantly of tremolite, serpentine, secondary magnetite, chlorite, and talc. Development of secondary minerals like serpentine and tremolite, replacing olivine and pyroxene requires gain/loss of MgO and SiO_2 to the bulk rock. A negative trend is observed between these two elements in the plot indicating alteration of MgO and or SiO_2 by secondary processes (Fig. 6). These mineral assemblages have been attributed to the varying degree of hydrothermal alteration and indicate greenschist to lower amphibolite facies of metamorphism. Most of the analysed samples show the consistency in Al_2O_3/TiO_2 and $(Gd/Yb)_N$ ratios and REE fractionation patterns. Mobility of major oxides and trace elements like SiO_2, CaO, Fe_2O_3, Al_2O_3, Na_2O and TiO_2, and P_2O_5, TiO_2, Co, Rb, and Y are noticed in this rock which is attributed by the presence of smooth fractionation patterns of major-element oxides and scattering patterns of trace elements (Fig. 6 & 7). In the primitive-mantle normalised multi-element spider diagram is also displaying crisscrossing of LILE indicative of their mobility (Fig. 8b). Komatiite samples do not display any significant Ce anomalies (Fig. 8a). Several studies have revealed that Ce anomalies occur in response to oxidation of Ce^{3+} to Ce^{4+} and precipitation of Ce^{4+} from solution as CeO_2 (Braun et al., 1993). The mild positive Ce anomaly noticed in some samples could probably be related to precipitation of Ce by the circulation of fluid phase in an oxidising condition, whereas the minor Ce depletion in some others observed could be attributed to the removal of Ce by circulating fluids during metamorphism. Analysed samples display strong negative Eu anomalies, implying that most magnesium-rich rocks were vulnerable to alteration (Lecuyer et al., 1994; Fan and Kerrich, 1997). Eu anomalies were also noticed in komatiites of the other cratons, which are generally attributed to secondary alteration (Sun and Nesbitt, 1978; Ludden et al., 1982; Arndt, 1994). Although the majority of the studied komatiites do not exhibit LREE enrichment and absence of Nb anomalies generally indicative of the absence of significant crustal contamination. Zr/Th, Nb/Th, Nb/U, Zr/Nb, and Nb/La ratios (Table 1) and strong positive U, Pb, and Y anomalies are attributed to some degree of crustal contamination (Fig. 8b).

Magmatic fractionation of trace elements

The komatiites show moderate to strong linear trends in binary diagrams (see Fig. 6 & 7) which is indicating that the source magmas evolved by differentiation processes. The positive correlation of MgO with Ni (Fig. 7) suggests that primary MgO contents were largely controlled by fractionation or accumulation of olivine. Negative trends of SiO_2, Al_2O_3, Fe_2O_3, Na_2O, Cr, Sc, V, and Zr with MgO indicate the possible involvement of olivine fractionation and garnet as a fractionating phase (Fig. 6 & 7). The majority of komatiite samples exhibits chondritic to sub-chondritic REE (7.45 - 55.32 ppm) patterns indicating their derivation from a depleted mantle source. The nature of sources and composition of melt residues have been identified by using the anomalies of Zr, Hf, and Y (Xie et al., 1993; Fan and Kerrich, 1997; Polat et al., 1999). Lahaye et al., 1995 and Polat et al., 1999 proposed that the Al-depleted komatiites from the Barberton greenstone belt have to be derived from the deep mantle melt segregation in a plume with residual majorite garnet at depths of 400 km based on strong negative Zr and Hf anomalies. Nb-anomalies on the primitive mantle normalised multi-element spider diagram has been used to characterise different mantle sources and also used as powerful tectonic discriminants between plume and arc settings (Jochum et al., 1991; Puchtel et al., 1997). Positive Nb-anomalies may suggest their derivation from the plume source that contains recycled slab material at greatest mantle depths (Kerrich and Xie, 2002). Polat and Kerrich, 2000 attributed that the negative Nb-anomalies reflect the generation of magma in arc environments or by crustal contamination processes. None of the samples of komatiite are showing anomalies of Nb while plotting in the primitive mantle normalised multi-element spider diagram (Fig. 8b) which is indicated that komatiite might be derived from a deep mantle plume source probably containing recycled slab component. The observed range of $(Gd/Yb)_N$ values, Zr and Y anomalies, and relatively flat HREE patterns reveals reflecting the magma generation at different depths melt generation at different depth (~250 - 350 km) in the mantle with or without the involvement of residual garnet.

Al-depletion and garnet fractionation

Nesbitt and Sun, 1976 and Sun, 1984 identified two main types of komatiites based on major oxides contents i.e. Al-depleted (Barberton komatiite) and Al-undepleted (Munro komaitte). Later on, Arndt, 2003 and Arndt et al., 2008 proposed a new classification for the komatiites: (i) the Barberton-type komatiites characterised by high CaO/Al_2O_3 (>1.0), low Al_2O_3/TiO_2 (<16) and depleted HREE; (ii) the Munro-type komatiites with lower CaO/Al_2O_3 (<1.0), higher Al_2O_3/TiO_2 (>20) and HREE; and (iii) the Gorgana-type komatiites with high Al_2O_3/TiO_2. Late Archaean to Proterozoic komatiites have Al_2O_3/TiO_2 ratios of around 20 (Arndt et al., 2008; Robin-Popieul et al., 2012), a value was close to the chondritic value and distinctly higher than that of the rocks of the Barberton greenstone belt (Nesbitt and Sun, 1976; Sun and Nesbitt, 1978; Nesbitt et al., 1979). The genesis of Al-depleted komatiite (Barberton-type komatiite) is attributed by the presence of garnet in the melt phase at a deeper level of the mantle (Jahn et al., 1982; Cattell and Arndt, 1987; Gruau et al., 1987; Xie et al., 1993; Arndt, 2003). A high degree of peridotite melting (~50%) at a shallower level is inferred the generation of Al-undepleted Munro type komatiites, where the mantle source intersected the solidus and garnet was removed from the residue before the melt acquired komatiitic composition. As per the experimental studies have been carried out by Ohtani et al. (1989) and Herzberg, (1999), the major element composition of Al-depleted komatiite melt is generated by partial melting of peridotite at pressures >8 GPa, whereas Al-undepleted komatiites formed during high degree melting of mantle peridotite at a shallow level. The ratios of CaO/Al_2O_3 and $(Gd/Yb)_N$ values have been used by Jahn et al., 1982 and Gruau et al., 1992 for the identification of garnet source in the melt phase. Presence of garnet as a residual phase in the mantle is supported by High CaO/Al_2O_3 (>1.0) and $(Gd/Yb)_N$ >1.0 and low CaO/Al_2O_3 (<1.0) and $(Gd/Yb)_N$ <1.0 indicative of garnet entering into the melt phase. Patka komatiite samples are characterised by Al-depleted with high CaO/Al_2O_3 ratios (>1.0), Al_2O_3/TiO_2 (8.65 - 30.47), and $(Gd/Yb)_N$ >1.0 suggesting the involvement of garnet as a residual phase. The ratios of CaO/Al_2O_3 > 1 are observed in those samples having high MgO contents (>30 wt. %) whereas samples with low MgO contents (<30 wt. %) have low CaO/Al_2O_3 ratios <1 (Table 1). Jahn et al., 1982 and Arndt, 2003 used the major element ratios such as CaO/Al_2O_3 and Al_2O_3/TiO_2 in combination with $(Gd/Yb)_N$ to identified the nature of mantle sources and garnet fractionation. In this study bivariate plots of $(Gd/Yb)_N$ versus CaO/Al_2O_3 and Al_2O_3/TiO_2 imply varying degrees of involvement of garnet in the generation of komatiite melt in the mantle (Fig. 8c & 8d).

Speculation on the possible tectonic setting and genesis of komatiite

The geodynamic context of komatiite magma generation and eruption has been a debated topic during the last four decades. The various concept has been proposed for the origin of komatiite magma includes: (i) they are related to mantle plume (Ohtani et al., 1989; Arndt et al., 1997; Kerrich and Xie, 2002; Arndt, 2003), (ii) genesis in oceanic plateaus originated from mantle plume (Kerr et al., 1996; Polat and Kerrich, 2000), (iii) formed in combined plume-arc setting (Puchtel et al., 1999; Jayananda et al., 2008) and (iv) genesis in subduction zone setting (Parman et al., 1997, 2001; Grove et al., 1999). Lateral accretion of crust in the subduction zone context is to be considered as a major process for the formation of Tonalite-trondhjemite-granodiorite (TTG) crust in the Archaean cratons (for review see Martin and Moyen, 2002; Smithies et al., 2003). The subduction zone model for the genesis of 3.45 Ga Barberton komatiites has been proposed by Parman et al., 1997 and 2001. The efficacy of an arc environment in accounting for the chemical characteristics of komatiites mainly Al-depletion, high-MgO, positive or absence of Nb anomalies, Nb/U, Nb/Th, Nb/La, and Th/U ratios and high eruption temperatures of Archaean komatiites (~ 1600ºC) has been debated (Arndt, 2003; Chavagnac, 2004; Jayananda et al., 2008). However, Mukhopadhyay et al. (2012) have inferred an oceanic supra-subduction zone geodynamic setting from their studies in the southern IOG mainly in the Tomka-Daitari belt. Many workers have suggested the origin of komatiite melt from the ascending hottest portions of mantle plumes (Campbell et al., 1989; Ohtani et al., 1989; Griffith and Campbell, 1992; Arndt et al., 1997; Arndt, 1994, 2003; Chavagnac, 2004; Jayananda et al., 2008).

ISSN: 2319-7064
ResearchGate Impact Factor (2018): 0.28 | SJIF (2019): 7.583

In the following section, we discuss various models to explain the tectonic setting of komatiite magma generation and eruption within the regional geological framework of the Singhbhum craton. Any geodynamic model proposed for Mesoarchean komatiites in BGGB must account for sub-contemporaneous mafic to felsic rocks of greenstone belt and the surrounding TTG basement. The analysed data of Patka komatiites are plotted in different discriminating diagrams viz. R_1 - R_2, Zr vs. Zr/Y, Zr vs. Ti, Zr/Nb, and Nb/Th and Nb/Y vs. Zr/Y for understanding the tectonic environments of komatiites. The plot of R_1 - R_2 diagram (Fig. 9a) point out the origin of komatiites through mantle-derived fractionates. Komatiites tend to plot in the field of island arc basalts in Zr vs. Zr/Y diagram (Pearce and Norry, 1979) and IAT field in Zr vs. Ti binary diagram (Pearce and Cann, 1973) (Figs. 9b & c). Data on the mafic-ultramafic volcanics (Sengupta et al., 1997) from eastern, western and southern segments of the IOG supracrustals in the Singhbhum craton were plotted together with the Patka komatiites in Nb/Th vs. Zr/Nb and Zr/Y vs. Nb/Y diagrams (Figs. 9d & e) which help a comparative study and speculation of the possible tectonic settings for these rocks (Fig. 1 of Condie, 2005). In the Nb/Th vs. Zr/Nb diagram, these komatiites cluster away from the other volcanics, and in the Nb/Y vs. Zr/Y diagram, they cluster between deep depleted mantle (DEP) and primitive mantle (PM). The Patka komatiite in the BGGB erupted in marine and sub-aerial environments and is enriched in SiO_2, MgO, Ni, and Cr but depleted in Al_2O_3 and TiO_2. Al_2O_3/TiO_2, CaO/Al_2O_3, $(Gd/Yb)_N$, $(Sm/Yb)_N$ and $(La/Sm)_N$ ratios, absent of Nb anomalies and LREE and HREE patterns indicate the derivation of these komatiites in a mantle plume - arc geodynamic setting with moderate contamination by continental crust or sub-continental lithosphere

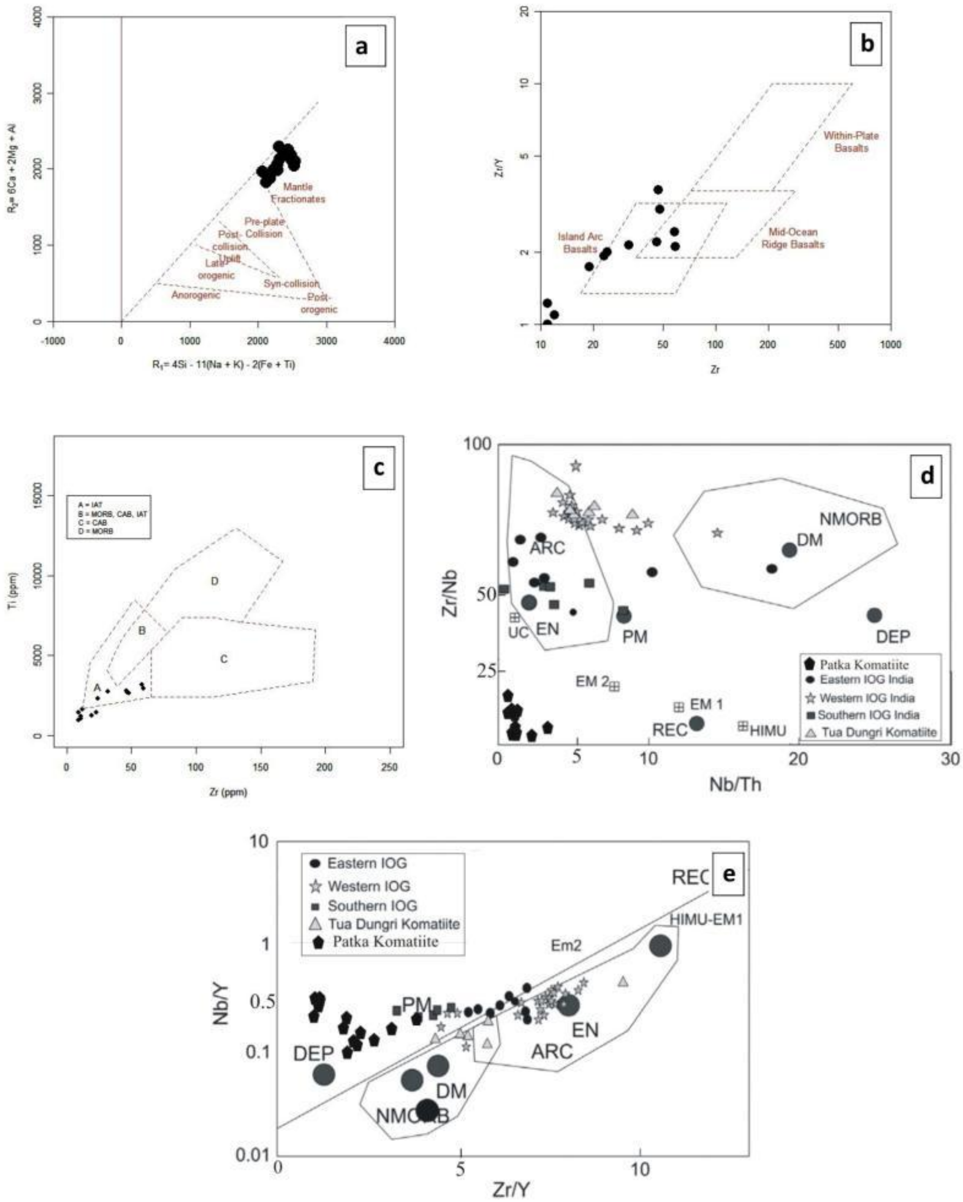

Figure 9: (a) Diagram of R_1 = 4Si-11(Na+K)-2(Fe+Ti) vs. R_2= 6Ca+2Mg+Al (Batchelor & Bowden, 1985) **(b)** Patka komatiites plotted in Zr vs. Zr/Y diagram (Pearce and Norry, 1979). **(c)** Zr vs. Ti binary after Pearce and Cann (1973). **(d and e)** Zr/Nb vs. Nb/Th and Nb/Y vs. Zr/Y plots of komatiites and other volcanic rocks of Iron Ore Group of different segments in the Singhbhum craton (see Fig. 1 of Condie, 2005).

(**Abbreviations:** IAT, island arc tholeiites; MORB, mid-ocean ridge basalts; CAB, continental arc basalts; WPB, within plate basalt; UC, upper continental crust; PM, primitive mantle; DM, shallow depleted mantle; HIMU, high mu (U/Pb) source; EM1 and EM2, enriched mantle sources; ARC, arc related basalts; NMORB, normal ocean ridge basalt; OIB, oceanic island basalt; DEP, deep depleted mantle; EN, enriched component; REC, recycled component).

3. Conclusion

Hitherto-unreported one body of komatiite from the Badampahar Group belonging to the eastern Iron Group, Singhbhum Craton is mapped to the south of Patka, Jharkhand which preserved excellent random spinifex, platy spinifex, and cumulate zones. It is mainly composed of tremolite, serpentine, magnetite, chlorite, and talc besides glass and rare skeletal olivine, clinopyroxene, and orthopyroxene minerals assemblage, indicative the metamorphism from greenschist to lower amphibolite facies. Komatiite is enriched in SiO_2, MgO, Ni, and Cr but depleted in Al_2O_3 and TiO_2. Al_2O_3/TiO_2, CaO/Al_2O_3, $(Gd/Yb)_N$, $(Sm/Yb)_N$ and $(La/Sm)_N$ ratios, absent of Nb anomalies and LREE and HREE patterns. In the Nb/Th vs. Zr/Nb diagram, these komatiites cluster away from the other volcanic, and in the Nb/Y vs. Zr/Y diagram, they cluster between deep depleted mantle (DEP) and primitive mantle (PM). Bivariate plots of $(Gd/Yb)_N$ versus CaO/Al_2O_3 and Al_2O_3/TiO_2 imply a varying degree of involvement of garnet in the generation of komatiite melt in the mantle. Based on the above observations, it can be stated that the derivation of Patka komatiite in a mantle plume - arc geodynamic setting with moderate contamination by continental crust or sub-continental lithosphere.

4. Acknowledgments

The authors express thanks to the Director General, Geological Survey of India for permitting publication of the paper and are also grateful to the Deputy Director General, SU: Odisha, Bhubaneswar for providing necessary logistics support while carrying out fieldwork and laboratory studies. The authors would like to convey their sincere thanks and gratitude to the Deputy Director General, SU: Bihar, Patna and Shri S. C. Srivastava, former Director, Geological Survey of India for their cooperation, constant encouragement, guidance and valuable suggestions during the work.

References

[1] Acharyya, S.K., Gupta, A. and Orihashi, Y., 2010: New U–Pb zircon ages from Palaeo-Mesoarchaean TTG gneisses of the Singhbhum Craton, eastern India. Geochem. J. 44, 81-88.
[2] Allegre, C.J., 1982: Genesis of Archaean komatiites in a wet ultramafic subducted plate. In: Arndt NT, Nisbet EG (eds) Komatiites. Springer-Verlag, Berlin, pp 495-500.
[3] Arndt, N.T., 1994: Archean komatiites. In: Condie, K.C. (Ed.), Archean Crustal Evolution. Elsevier, Amsterdam, pp. 11-44.
[4] Arndt, N.T., 2003: Komatiites, kimberlites, and boninites. J. Geophys. Res.108, 2293.
[5] Arndt, N.T., 2008: Komatiite, first ed. Cambridge University Press, New York.
[6] Arndt, N.T., Albarede, F. and Nisbet, E.G., 1997: Mafic and ultramafic magmatism. In: De Wit, M.J., Ashwal, L.D. (Eds.), Greenstone Belts. Oxford University Press, Oxford, pp. 233-254.
[7] Arndt, N.T., Ginibre, C., Chauvel, C., Albarede, F., Cheadle, M., Herzberg, C., Jenner, G. and Lahaye, Y., 1998: Were komatiites wet? Geology 26: 739-742.
[8] Arndt, N.T. and Nisbet, E.G., 1982: What is a komatiite? In: Arndt, N.T., Nisbet, E.G. (Eds.), Komatiites. George Allen and Unwin, London, pp. 19-28.
[9] Arndt, N.T., Lesher, C.M. and Barnes, S.J., 2008: Komatiite. Cambridge University Press.
[10] Batchelor, R.A. and Bowden, P., 1985: Petrogenetic interpretation of granitoid rock series using multicationic parameters. Chemical Geology, 48, 43-55.
[11] Berry, A.J., Danyashevsky, L.V., O'Neill, Hugg St.C., Newville, M. and Sutton, S.R., 2008: Oxidation state of iron in komatiite melt inclusions indicates hot Archean mantle. Nature 455, 960-963.
[12] Banerjee, A.K. 1974: On the stratigraphy and tectonic history of the iron ore bearing and associated rocks of Singhbhum and adjacent areas of Bihar and Orissa, Jour. Geol. Soc. Ind., v. 15 (2), pp. 150-157.
[13] Bhattacharya, U., Ghosh, D.K., Sen, P. and Chakrabarti, R., 1996: Spinifex textured komatiite from Archaean greenstone sequence of Singhbhum District, eastern India. Jour. Geol. Soc. India, v.48, pp. 357-461.
[14] Bickle, M.J., Arndt, N.T., Nisbet, E.G., Orpen, J.L., Martin, A., Keays, R.R. and Renner, R., 1993: Geochemistry of the igneous rocks of the Belingwe greenstone belt: alteration, contamination and petrogenesis. In: Bickle, M.J., Nisbet, E.G. (Eds.), the Geology of the Belingwe Greenstone Belt, Zimbabwe: A Study of the Evolution of Archaean Continental Crust. A.A. Balkema, Rotterdam, pp. 175-214.
[15] Boehler, R., Chopelas, A. and Zerra, A., 1995: Temperature and chemistry of the core-mantle boundary. Chem. Geol. 120: 199-205.
[16] Bose, M.K., 2009: Precambrian mafic magmatism in the Singhbhum Craton, eastern India. J. Geol. Soc. India, 73, 13-35.
[17] Braun, J.J., Pagel, M., Herbillon, A. and Rosin, C., 1993: Mobilization and redistribution of REEs and thorium in a syenitic lateritic profile: A mass balance study. Geochimica et Cosmochimica Acta 57, 4419-4434.
[18] Campbell, I.H., Griffiths, R.W. and Hill, R.I., 1989: Melting in an Archaean mantle plume: heads its basalts, tails its komatiites. Nature 339, 697-699.
[19] Cattell, A. and Arndt, N., 1987: Low and high alumina komatiites from a late Archaean sequence,

Newton Township, Ontario. Contrib. Miner. Petrol. 97, 218-227.

[20] Charan, S.N., Naqvi, S.M. and Ramesh, S.L., 1988: Geology and geochemistry of spinifex-textured peridotitic komatiite from Mayasandra schist belt, Karnataka. Jour. Geol. Soc. India, v.44, pp. 483-493.

[21] Chaudhuri, T., Mazumder, R. and Arima, M., 2015: Petrography and geochemistry of Mesoarchaean komatiites from the eastern Iron Ore belt, Singhbhum craton, India, and its similarity with 'Barberton type komatiite'. Jour. Africa. Earth Sci. (101) 135-147.

[22] Chaudhuri, T., Satish, M. Mazumder, and Biswas, S. 2017: Geochemistry and Sm-Nd isotopic characteristics of the Paleoarchean Komatiites from Singhbhum Craton, Eastern India and their implications. Precambrian Research, 298: 385-402.

[23] Chavagnac, V., 2004: A geochemical and Nd isotopic study of Barberton komatiites (South Africa): implication for the Archean mantle. Lithos 75, 253-281.

[24] Condie, K.C., 2005. High field strength element ratios in Archean basalts: a window to evolving sources of mantle plumes? Lithos 79, 491-504.

[25] Devapriyan, G.V., Anantharamu, T.R., Vidyadharan, K.T. and Raghunandan, K.R., 1994: Spinifex-textured peridotitic komatiite from Honnabetta area, Nagamangala schist belt, Karnataka. Jour. Geol. Soc. India, v.44, pp. 483-493.

[26] De Wit, M.J. and Ashwal, L.D., 1997: Preface: convergence towards divergent models of greenstone belts. In: de Wit, M.J., Ashwal, L.D. (Eds.), Greenstone Belts. Oxford University Press, Oxford, pp. 9-17.

[27] Dostal, J. and Mueller, W.U., 2012: Deciphering an Archean Mantle Plume: Abitibi Greenstone Belt, Canada. Gondwana Research. http://dx.doi.org/10.1016/j.gr.2012.02.2015.

[28] Dunn, J. A. 1929: Geology of north Singhbhum including parts of Ranchi and Mayurbhanj districts. Mem Geol Surv India; 54: 1-166.

[29] Fan, J. and Kerrich, R., 1997: Geochemical characteristic of Al-depleted and undepleted komatties and HREE-enriched tholeiites, western Abitit greenstone belt: variable HFSE/REE systematic in a heterogeneous mantle plumes. Geochimicaet Cosmochimica Acta 61, 4723-4744.

[30] Furnes, H., de Wit, M. and Robins, B., 2012: A Review of New Interpretations of the Tectonostratigraphy, Geochemistry and Evolution of the Onverwacht Suite, Barberton Greenstone Belt, South Africa. Gondwana Research. http://dx.doi.org/10.1016/j.gr.2012.02.2015.

[31] Goswami, J.N., Mishra, S., Wiedenbeck, M., Ray, S.L. and Saha, A.K., 1995: $207^{Pb}/206^{Pb}$ ages from the OMG, the oldest recognized rock unit from Singhbhum-Orissa Iron Ore craton, E. India. Curr. Sci. 69, 1008-1012 (Bangalore).

[32] Griffith, R.W. and Campbell, I.H., 1992: On the dynamics of long-lived plume conduits in the convecting mantle. Earth Planet. Sci. Lett. 103, 214-227.

[33] Grove, T.L., deWit, M.J. and Dann, J., 1997. In: dewit, M.J., Ashwal, L.D. (Eds.): Komatiites from the Komati Type Section, Barberton, South Africa, in Greenstone Belts. Oxford Science, Oxford, U.K., pp. 422-437.

[34] Grove, T.L., Parman, S.W. and Dann, J.C., 1999: Condition of magma generation for Archaean komatiites from the Barberton Mountain Land, South Africa. In: Fei, Y., Bertal, C.M., Mysen, B.O. (Eds.), Mantle Petrology: Field Observations and High Pressure Experimentation. The Geochemical Society, Candmus Journal Services, Lancaster, pp. 155-167.

[35] Grove, T.L. and Parman, S. W., 2004: Thermal evolution of the earth as recorded by komatiites. Earth Planet Sci. Lett. 219: 173-187.

[36] Gruau, G., Jahn, B.M., Glikson, A.Y., Davy, R., Hickman, A.H. and Chauvel, C., 1987: Age of the Talga–Talga Subgroup, Pilbara Block, Western Australia, and early evolution of the mantle: new Sm–Nd isotopic evidence. Earth Planet. Sci. Lett. 85, 105-116.

[37] Gruau, G., Toupin, S., Fourcade, S. and Blais, S., 1992: Loss of (Nd, O) and chemical (REE) memory during metamorphism of komatiites: new evidence from eastern Finland. Contribution to Mineralogy and Petrology 112, 66-82.

[38] Herzberg, C., 1995: Generation of plume magmas through time: an experimental perspective. Chem. Geol. 126, 1-16.

[39] Herzberg, C., 1999: Phase equilibrium constraints on the formation of cratonic mantle. In: Fei, Y., Bertka, C.M., Mysen, B.O. (Eds.), Mantle Petrology: Field Observations and High-pressure Experimentation, vol.6 Special Publication, Geochemical Society, pp. 241-257.

[40] Hussain, M. and Naquvi, S.M., 1983: Geological, geophysical and geochemical studies over the Holenarsipur schist belt, Dharwar craton, India. In Naqvi, S. M., and Rogers, J. J. W., eds. Precambrian of south India. Geol. Suv. India, Mem. 4, pp 73-95.

[41] Iyenger, S.V.P. and Murthy, Y.G.K. 1982: The evolution of the Archaean-Proterozoic Crust in parts of Bihar and Orissa, Eastern India, Geol. Sur. India, Rec., v.112 (3), pp.1-6.

[42] Jahn, B.M., Gruau, G. and Glickson, A.Y., 1982: Komatiites of the Onverwacht Group, South Africa: REE chemistry, Sm–Nd age and mantle evolution. Contrib. Miner. Petrol. 80, 25-40.

[43] Jayananda, M., Kano, T., Peucat, J.J. and Channabasappa, S., 2008: 3.35 Ga komatiite volcanism in the western Dharwar craton, southern India: constraints from Nd isotopes and whole-rock geochemistry. Precambr. Res. 162, 160-179.

[44] Jena, B.K. and Mohanty, A.M. 1989: Some significant finds from Orissa. News, Eastern Region, GSI., v.9, pp.8-9.

[45] Jena, B.K. and Behera, U.K. 1998: The oldest supracrustals belt from Singhbhum craton and its possible correlation. Precambrian Crust in Eastern and Central India, Proceedings of the international seminar UNESCO-IUGS-368, Geo. Sur. Ind., Speci. Pub., v.57, pp.106-121.

[46] Jochum, K.P., Arndt, N.T. and Hofmann, A.W., 1991: Nb-Th-La in komatiites and basalts: constraints on

komatiites Petrogenesis and mantle evolution. Earth Planet. Sci. Lett. 107, 272-289.

[47] Jones, H.C. 1934: The iron ore deposits of Bihar and Orissa. Mem. Geol. Surv. India, V.63, pp.357.

[48] Kerr, A.C., Marriner, G.F., Arndt, N.T., Tarney, J., Nivia, A., Saunders, A.D. and Duncan, R., 1996: The Petrogenesis of Gorgona komatiites, picrites and basalts: new field, petrographic and geochemical constraints. Lithos 37, 245-260.

[49] Kerrich, R., Wyman, D., Hollings, P. and Polat, A., 1999: Variability of Nb/Th and Th/La in 3.0 to 2.7 Ga Superior province ocean plateau basalts: implications for the timing of continental growth and lithosphere recycling. Earth and Planetary Science Letters 168, 101-115.

[50] Kerrich, R. and Xie, Q., 2002: Compositional recycling structure of an Archaean super-plume: Nb-Th-U-LREE systematic of Archaean komatiites and basalts revisited. Contribution to Mineralogy and Petrology 142, 476-484.

[51] Lahaye, X., Arndt, N.T., Byerly, G., Chauvel, C., Fourcade, S. and Gruau, G., 1995: The influence of alteration on teh trace-element and Nd isotopic compositions of Komatiites. Chem. Geol. 126, 43-64.

[52] Lahaye, Y. and Arndt, N.T., 1996: Alteration of a komatiitic flow: Alexo, Ontario, Canada. J. Petrol. 37, 1261-1284.

[53] Le Bas, M.J., 2000: IUGS reclassification of the high-Mg and picritic volcanic rocks. J.Petrol. 41, 1467-1470.

[54] Lecuyer, C., Gruau, G., Anhaeusser, C.R., Fourcade, S. and Gruau, G., 1994: The origin of fluids and the effect of metamorphism on the primary chemical compositions of Barberton komatiites; new evidence from geochemical (REE) and isotopic (Nd, O, H, $^{39}Ar/^{40}Ar$) data. Geochim. Cosmochim. Acta 58, 969-984.

[55] Lesher, C.M. and Arndt, N.T., 1995: REE and Nd isotope geochemistry, petrogenesis and volcanic evolution of contaminated komatiites at Kambalda, Western Australia. Lithos 34, 127-157.

[56] Ludden, J.N., Gelinas, L. and Trudel, P., 1982: Archaean metavolcanics from the Rouyn-Noranda district, Abitibi greenstone belt, Quebec. 2. Mobility of trace elements and Petrogenetic constraints. Can. J. Earth Sci. 19, 2276-2287.

[57] Martin, H. and Moyen, J.F., 2002: Secular change in tonalite-trondhjemite-granodiorite composition as markers of the progressive cooling of earth. Geology 30(4), 319-322.

[58] Mazumder, R., Eriksson, P.G., De, S., Bumby, A.J. and Lenhardt, N., 2012a: Palaeoproterozoic sedimentation on the Singhbhum craton: global context and comparison with Transvaal. In: Mazumder, R., Saha, D. (Eds.), Palaeoproterozoic of India, vol. 365. Geological Society, London, pp. 49-74 (Special Publication).

[59] Mazumder, R., Van Loon, A.J., Mallik, L., Reddy, S.M., Arima, M., Altermann, W., Eriksson, P.G. and De, S., 2012b. Mesoarchaean–Palaeoproterozoic stratigraphic record of the Singhbhum crustal province, eastern India: a synthesis. In: Mazumder, R., Saha, D. (Eds.), Palaeoproterozoic of India, vol. 365. Geological Society, London, pp. 29-47, Special Publication.

[60] Misra, S., Deomurari, M.P., Wiedenbeck, M., Goswami, J.N., Ray, S. and Saha, A.K., 1999: $^{207}Pb/^{206}Pb$ zircon age ages and the evolution of the Singhbhum craton, eastern India: an ion microprobe study. Precambrian Research 93, 139-151.

[61] Misra, S., 2006: Precambrian chronostratigraphic growth of Singhbhum-Orissa Craton, eastern Indian Shield: an alternative model. J. Geol. Soc. India 67, 356-378.

[62] Mukhopadhyay, D., 2001: The Archean nucleus of Singhbhum: the present state of knowledge. Gondwana Res. 4, 307-318.

[63] Mukhopadhyay, J., Beukes, N.J., Armstrong, R.A., Zimmermann, U., Ghosh, G. and Medda, R.A., 2008: Dating the oldest greenstone in India: A 3.51 Ga precise U–Pb SHRIMP zircon age for dacitic lava of the Southern Iron Ore Group, Singhbhum Craton. J. Geol. 116, 449-461.

[64] Mukhopadhyay, J., Ghosh, G., Zimmermann, U., Guha, S. and Mukherjee, T., 2012: A 3.51 Ga bimodal volcanics-BIF-ultramafic succession from Singhbhum Craton: implications for Palaeoarchaean geodynamic processes from the oldest greenstone succession of the Indian subcontinent. Geol. J. 47, 284-311.

[65] Nakamura, N. 1974: Determination of REE, Ba, Fe, Mg, Na and K in carbonaceous and ordinary chondrites, Geochim. et Cosmochim. Acta, 38, 757-775.

[66] Nelson, D.R., Bhattacharya, H.N., Thern, E.R. and Altermann, W. 2014: Geochemical and ion-microprobe U–Pb zircon constraints on the Archaean evolution of Singhbhum Craton, eastern India. Precamb. Res. (Accepted manuscript).

[67] Nesbitt, R.W. and Sun, S.S., 1976: Geochemistry of Archaean spinifex-textured peridotites and magnesian and low-magnesian tholeiites. Earth Planet. Sci. Lett. 31, 433-453.

[68] Nesbitt, R.W., Sun, S.S. and Purvis, A.C., 1979: Komatiites: geochemistry and genesis. Can. Mineral. 17, 165-186.

[69] Nesbitt, R.W., Jahn, B.M. and Purvis, A.C., 1982: Komatiites: an early Precambrian phenomenon. J. Volcanol. Geoth. Res. 14, 31-45.

[70] Nisbet, E.G., Cheadle, M.J., Arndt, N.T. and Bickle, M.J., 1993: Constraining the potential temperature of the Archaean mantle: a review of the evidence from komatiites. Lithos 30, 291-307.

[71] Ohtani, E., Kawabe, I., Moriyama, J. and Nagata, Y., 1989: Partitioning of elements between majorite garnet and melt and implications for petrogenesis of komatiite. Contrib. Miner. Petrol. 103, 263-269.

[72] Parman, S.W., Dann, J.C., Grove, T.L. and de Wit, M.J., 1997: Emplacement conditions of komatiite magmas from the 3.49 Ga Komati Formations, Barberton greenstone belts, South Africa. Earth and Planetary Science Letters 150, 303-323.

[73] Parman, S.W., Grove, T.L. and Dann, J.C., 2001: The production of Barberton komatiites in an Archaean subduction zone. Geophysical Research Letters 28, 2513-2516.

[74] Pearce, J.A. and Cann, J.R., 1973: Tectonic setting of basic volcanic rocks determined using trace element analysis. Earth Planet Sci Lett 19: 290-300.

[75] Pearce J. A. and Norry, M. J. 1979: Petrogenetic implications of Ti, Zr, Y and Nb variations in volcanic rocks. Contributions to mineralogy and petrology 69, 33-47.

[76] Polat, A., Kerrich, R. and Wyman, D.A., 1999: Geochemical diversity in oceanic komatiites and basalts from the late Archean Wawa greenstone belts, Superior Province, Canada: trace element and Nd isotope evidence for a heterogeneous mantle. Precambrian Research 94, 139-173.

[77] Polat, A. and Kerrich, R., 2000: Archaean greenstone belt magmatism and the continental growth-mantle evolution connection: constraints from Th-U-Nb-LREE systematic of the 2.7 Ga Wawa subprovince, Superior province, Canada Earth and Planetary Science Letters 175, 41-54.

[78] Puchtel, I.S., Hasee, K.M., Hofmann, A.W., Chauvel, C., Kulikov, V.S., Garbe-Schonberg, C.D. and Nemchin, A.A., 1997: Petrology and geochemistry of crustally contaminated komatitic basalts from the Vetreny Belt, south-eastern Baltic continental lithosphere. Geochimica et Cosmochimica Acta 61, 1205-1222.

[79] Puchtel, I.S., Hofmann, A.W., Amelin, Y.V., Garbe-Schonberg, C.D., Samsonov, A.V. and Shchipansky, A.A., 1999: Combined mantle plume-island arc model for the formation of the 2.9 Ga sumo-zero-kenozero greenstone belt, SE Baltic shield: isotope and trace element constrainsts. Geochimica et Cosmochimica Acta 63, 3579-3595.

[80] Radhakrishna, B.P. and Naqvi, S.M., 1986: Precambrian continental crust of India and its evolution. The Jour. Geo. Surv. India. vol. 94, No.2, pp 145-166.

[81] Raul Minas, K. and Jost, H., 2006: Low and high-alumina komatiites of Goias, Central Brazil, Journal of South America Earth Science 20, 315-326.

[82] Robin-Popieul, C.C.M., Arndt, N.T., Chauvel, C., Byerly, G.R., Sobolev, A.V., and Wilson, A., 2012: A new model for Barberton komatiites: deep critical melting with high melt retention. J. Petrol. 53, 2191–2229.

[83] Saha, A.K., 1994: Crustal evolution of Singhbhum-North, Orissa, eastern India. Geol. Soc. India Mem., 27.

[84] Sahu, N.K. and Mukherjee, M.M., 2001: Spinifex Textured Komatiite from Badampahar-Gorumahisani Schist Belt, Mayurbhanj District, Orissa. Jour. Geol. Soc. India, v.57, pp 529-534.

[85] Sahoo, K.C., Srivastava, S.C. and Mahakul, J.P. 2010: Specisiled Thematic Mapping around Bisoi-Manada-Betjharan area of Badampahar-Gorumahisani belt in Mayurbhanj district, Odisha. Unpublished Progress Report of GSI.

[86] Sarkar, S. N. and Saha, A. K. 1977: The present status of the Precambrian stratigraphy, tectonics geochronology of Singhbhum-Keonjhar-Mayurbhanj region, Eastern India. Ind.Jour. East. Sc. S. Ran. Vol. pp 37-43.

[87] Sengupta, S., Acharyya, S.K. and De Smith, J.B., 1997: Geochemistry of Archaean volcanic rocks from Iron Ore Supergroup, Singhbhum, eastern India. Proc. Indian Acad. Sci. (Earth Planet. Sci.) 106, 327-342.

[88] Smithies, R.H., Champion, D.C. and Cassidy, K.F., 2003: Formation of Earths early Archaean continental crust. Precambrian Research 127, 89-101.

[89] Srikantia, S.V. and Bose, S.S., 1985: Archaean komatiites from Banasandra area of Kibbanahalli arm of Chitradurga Supracrustal belt in Karnataka. J. Geol. Soc. India 26, 407-417.

[90] Subba Rao, D.V. and Naqvi, S.M., 1999: Archaean Komatiites from the older schist belt of Kalyadi in Western Dharwar craton, Karnataka. J. Geol. Soc. India 53, 347-354.

[91] Sun, S.S. and Nesbitt, R.W., 1978: Petrogenesis of Archean ultrabasic and basic volcanics: evidence from rare earth elements. Contrib. Miner. Petrol. 65, 301-325.

[92] Sun, S.S., 1984: Geochemical characteristics of Archaean ultramafic and mafic volcanic rocks: implications for mantle composition and evolution, In: Kroner, A., Goodwin, A. M., Hanson, G. N., (Eds.), Archaean Geochemistry. Springer-Verlag, Berlin, pp, 25-46.

[93] Sun, S.S. and McDonough, W.F., 1989. Chemical and isotopic systematics of oceanic basalts: implications for mantle composition and processes. In: Saunders, A.D., Norry, M.J. (Eds.), Magmatism in the Ocean Basins, vol. 42. Geological Society, London, pp. 313-345 (Special Publications).

[94] Sylvester, P.J., Harper, G.D., Byerly, G.R. and Thurston, P.C., 1997. Volcanic aspects. In: de Wit, M.J., Ashwal, L.D. (Eds.), Greenstone Belts. Oxford University Press, Oxford, pp. 55-90.

[95] Tait, J., Zimmermann, U., Miyazaki, T., Presnyakov, S., Chang, Q., Mukhopadhyay, J. and Sergeev, S., 2011: Possible juvenile Palaeoarchaean TTG magmatism in eastern India and its constraints for the evolution of the Singhbhum craton. Geol. Mag.148 (2), 340-347.

[96] Tourpin, S., Gruau, G., Blais, S. and Fourcade, S., 1991: Resetting of REE and Nd and Sr isotope during carbonitisation of a komatiite flow from Finland. Chemical Geology 90, 15-29.

[97] Tushipokla. and Jayananda, M. 2013: Geochemical constraints on komatiite volcanism from Sargur Group Nagamangala greenstone belt, western Dharwar craton, southern India: Implications for Mesoarchean mantle evolution and continental growth. Geosci. Fron. 4, 321-340.

[98] Upadhyaya, D., Chattopadhyaya, S., Kooijmanb, E., Mezgerc, K. and Berndt, J. 2014: Magmatic and metamorphic history of Paleoarcheantonalite–trondhjemite–granodiorite (TTG) suite fromthe Singhbhum craton, eastern India. Precamb. Res. 252, 180-190.

[99] Venkatadasu, S.P., Ramakrishnan, M. and Mahabaleswar, B., 1991: Sargur-Dharwar relationship around Komattite-rich rocks in Jayachamarajapura schist belt, Karanataka. Jour. Geol. Soc. India, v.38, pp. 577-592.

[100] Viljoen, M.J. and Viljoen, R.P., 1969a: Archaean volcanity and continental evolution in the Barberton region, Transvaal. In: Clifford, T.N., Gass, I. (Eds.), African Magmatism and Tectonics. Oliver and Boyd, Edinburgh, pp. 27-39.
[101] Viljoen, M.J., Viljoen, R.P. and Pearton, T.N., 1982: In Arndt, N. T., Nisbet, E. G. (Eds.), the Nature and Distribution of Archaean Komatiite Volcanics in South Africa. Komatiites, Allen and Unwin, London, pp. 53-79.
[102] Viswanatha, M.N., Ramakrishnan, M. and Narayana Kutty, T.R., 1977: Possible spinifex texture in a serpentinite from Karnataka. J. Geol. Soc. India 18, 194-197.
[103] Wilson, A.H. and Carlson, R.W., 1989: A Sm-Nd and Pb isotope study of Archaean greenstone belts in the Southern Kaapvaal Craton, South Africa. Earth and Planetary Science Letters 96, 89-105.
[104] Xie, Q., Kerrich, R. and Fan, J., 1993: HFSE/REE fractionations recorded in three komatiite-basalt sequences, Archean Abitibi greenstone belt: implications for multiple plume sources and depths. Geochim. Cosmochim. Acta 57, 4111-4118.
[105] Xie, H., Hofmann, A., Hegner, E., Wilson, A., Wan, Y. and Liu, D., 2012: Zircon SHRIMP dating confirms a Paleoarchean supracrustals terrain the southeastern Kaapvaal Craton, South Africa. Gondwana Research 21, 818-828.
[106] Yadav, P.K., Pradhan, U.K., Mukherjee, A., Sar, R.N., Sahoo, P. and Das, M., 2015: Basic characterization of Kapili Komatiite from Badampahar-Gorumahisani Schist Belt, Singhbhum Craton, Odisha, India. Jour. Geosci. India, 69 (1), 1-12.
[107] Yadav, P.K., Sahoo, P., Pradhan, U.K. and Das, M., 2016: Komatiite from Mesoarchaean Badampahar-Gorumahisani greenstone belt, Singhbhum craton, eastern India: Petrogenetic affinity with 'Barberton type'. 35th Inter.Geosci.Congress., Cape Town, South Africa.
[108] Yadav, P.K., Chaudhuri, T. and Das, A., 2016: Final Report on the Specialised Thematic Mapping in the transect between Luhakorha and Karanjia in the central part of Singhbhum Craton, Kendujhar district, Odisha. Unpublished Report of the Geological Survey of India, F.S. 2014-16.
[109] Yadav, P.K. and Das, M., 2017a: Petrology, geochemistry and petrogenesis of Al-depleted komatiite from Badampahar-Gorumahisani Greenstone Belt of Eastern Iron Ore Group, Singhbhum Craton, India. Jour. Geosci. India, 70 (3&4), 71 (1), 313-328.
[110] Yadav, P.K. and Das, M., 2017b: Geochemistry of Kapili Komatiite from Badampahar-Gorumahisani greenstone belt, Singhbhum craton, India and its resemblance with 'Barberton Komatiite'. Inter. Jour. Res. Analy. Reviews, V.4(4), 495-507.
[111] Yadav, P.K. 2017c: Incidence of uranium and thorium mineralization in quartz-pebble conglomerate of Koira Group, Singhbhum Craton, India. International Journal of Research and Analytical Reviews, 4(4): 484-488.
[112] Yadav, P.K. and Das, M., 2019a: Geochemistry of Mesoarchaean felsic tuff from Bonai-Kendujhar belt of Western Iron Ore Group, Singhbhum Craton, India: implications for volcanic arc tectonic setting. Indian Journal of Geosciences, 73(1): 1-14.
[113] Yadav, P.K. and Das, M., 2019b: Anomalous high values of rare earth element in quartz-pebble conglomerate of Koira Group of Western Iron Ore Group, Singhbhum Craton, India. Indian Journal of Geosciences, 73(2): 131-142.
[114] Yadav, P.K., Das, M. and Ray, S., 2020: Petrochemical signatures of meta-andesite from Badampahar-Gorumahisani Greenstone Belt, Singhbhum Craton: Implication on Precambrian tectonic setting of the Eastern India Shield. Indian Journal of Geosciences, 74(1): 33-55.
[115] Zhai, M.G. and Santosh, M., 2011: The early Precambrian odyssey of the North China Craton; a synoptic overview. Gondwana Research 20, 6-25.